



## Quantifying Arctic ozone loss during the 2004–2005 winter using satellite observations and a chemical transport model

C. S. Singleton,<sup>1</sup> C. E. Randall,<sup>1</sup> V. L. Harvey,<sup>1</sup> M. P. Chipperfield,<sup>2</sup> W. Feng,<sup>2</sup> G. L. Manney,<sup>3,4</sup> L. Froidevaux,<sup>3</sup> C. D. Boone,<sup>5</sup> P. F. Bernath,<sup>5</sup> K. A. Walker,<sup>5</sup> C. T. McElroy,<sup>6,7</sup> and K. W. Hoppel<sup>8</sup>

Received 2 May 2006; revised 8 August 2006; accepted 21 August 2006; published 4 April 2007.

[1] During the last decade, much attention has been placed on quantifying and modeling Arctic stratospheric O<sub>3</sub> loss. At issue in particular is the reliability of models for simulating the loss under variable dynamical conditions in the Arctic region. This paper describes inferred O<sub>3</sub> loss calculations for the 2004–2005 Arctic winter using data from four solar occultation satellite instruments, as well as the Earth Observing System Microwave Limb Sounder (EOS MLS). O<sub>3</sub> loss is quantified with the “Chemical Transport Model (CTM) passive subtraction” approach, using a passive O<sub>3</sub> tracer field from the SLIMCAT CTM. The 2004–2005 Arctic winter was moderately active dynamically, but was still one of the coldest Arctic winters on record, with prime conditions for O<sub>3</sub> loss. Loss estimates inferred from all of the different satellite instruments peaked in mid-March at 450 K between 2–2.3 ppmv, slightly less than similar estimations for the cold 1999–2000 winter. The SLIMCAT CTM was also used to simulate O<sub>3</sub> for the 2004–2005 winter. In March, near 450 K, the model O<sub>3</sub> was 0.3 ppmv (~10–15%) lower than the observations, leading to a maximum O<sub>3</sub> loss that was 10–15% larger than that inferred from observations, using the passive subtraction approach. Modeled loss maximized around the same time as that inferred from observations. Although some discrepancies between the observed and modeled O<sub>3</sub> remain, the level of agreement presented here shows that the SLIMCAT CTM was able to satisfactorily simulate O<sub>3</sub> and polar O<sub>3</sub> loss during the dynamically active 2004–2005 Arctic winter.

**Citation:** Singleton, C. S., et al. (2007), Quantifying Arctic ozone loss during the 2004–2005 winter using satellite observations and a chemical transport model, *J. Geophys. Res.*, 112, D07304, doi:10.1029/2006JD007463.

### 1. Introduction

[2] Since the discovery of the Antarctic O<sub>3</sub> hole in 1985 [Farman *et al.*, 1985], modeling O<sub>3</sub> loss has been an important focus of research in the atmospheric science community. At issue most recently is the feedback between climate change and stratospheric O<sub>3</sub> levels. In order to

predict changes in climate, scientists have employed coupled Chemistry Climate Models (CCMs). An integral part of developing CCMs is defining the most appropriate atmospheric chemistry modules, which should ideally be derived from chemical transport models (CTMs). CTMs are forced with winds and temperatures derived from analyses of observed meteorological parameters; therefore they cannot be used to make projections about future climate. However, CTMs are used to simulate present day atmospheric conditions and can be compared to observations to test our understanding of atmospheric phenomena. Previous studies have shown that CTMs have underestimated Arctic chemical O<sub>3</sub> loss compared to observed loss [Chipperfield *et al.*, 1996; Deniel *et al.*, 1998; Becker *et al.*, 2000; Guirlet *et al.*, 2000], which implies a gap in our understanding of O<sub>3</sub> loss processes. WMO [2003] states that “global CTMs reproduce a large fraction (60 to 100%, depending on the winter) of the observed O<sub>3</sub> loss in the Arctic and its variability”; however, uncertainties exist because of the “current unrealistic representation of denitrification processes in 3-D CTMs and unexplained O<sub>3</sub> losses during cold Arctic Januarys”. The report also states that, “these uncertainties prevent reliable predictions of future Arctic O<sub>3</sub> losses in a potentially changing climate [WMO, 2003].” Therefore in

<sup>1</sup>Laboratory for Atmospheric and Space Physics, UCB 392, University of Colorado, Boulder, Colorado, USA.

<sup>2</sup>Institute for Atmospheric Science, School of Earth and Environment, University of Leeds, Leeds, UK.

<sup>3</sup>Jet Propulsion Laboratory, California Institute of Technology, Pasadena, California, USA.

<sup>4</sup>Also at Department of Physics, New Mexico Institute of Mining and Technology, Las Vegas, New Mexico, USA.

<sup>5</sup>Department of Chemistry, University of Waterloo, Waterloo, Ontario, Canada.

<sup>6</sup>Meteorological Service of Canada, Environment Canada, Downsview, Ontario, Canada.

<sup>7</sup>Also at Department of Physics, University of Toronto, Toronto, Ontario, Canada.

<sup>8</sup>Naval Research Laboratory, Remote Sensing Physics Branch, Washington, D.C., USA.

order to correctly develop CCMs to make accurate predictions about future climate, it is imperative for CTMs to simulate changes in the stratospheric O<sub>3</sub> layer accurately.

[3] Recent studies have shown that changes made to CTMs have now improved their ability to simulate Arctic O<sub>3</sub> loss, even during complex, dynamically active winters [e.g., *Feng et al.*, 2005]. *Singleton et al.* [2005] have shown that during the 2002–2003 Arctic winter the SLIMCAT CTM was able to simulate O<sub>3</sub> loss that was inferred from Polar Ozone and Aerosol Measurement (POAM) III observations. In order to rigorously evaluate SLIMCAT or any other CTM for reliability in simulating Arctic O<sub>3</sub> loss processes, it is necessary to investigate multiple Arctic winters, since there is large interannual variability due to complex dynamical activity [WMO, 2003]. This paper describes inferences of chemical O<sub>3</sub> loss from observations (hereafter referred to as the inferred O<sub>3</sub> loss) inside the polar vortex for the 2004–2005 Arctic winter (defined here as the time period from 1 December 2004 to 1 April 2005) using a version of the well-validated “passive subtraction” technique [e.g., *Harris et al.*, 2002; WMO, 2003; *Manney et al.*, 1995a, 1995b, 2003; *Singleton et al.*, 2005]. Calculations of inferred O<sub>3</sub> loss in the lower stratosphere are shown at discrete levels and for the integrated partial column. Data from five different satellite instruments are used, including POAM III, the Stratospheric Aerosol and Gas Experiment (SAGE) III, the Earth Observing System Microwave Limb Sounder (EOS MLS), and the Atmospheric Chemistry Experiment Fourier Transform Spectrometer (ACE-FTS) and Measurement of Aerosol Extinction in the Stratosphere and Troposphere Retrieved by Occultation (MAESTRO). Inferred O<sub>3</sub> loss during the 2004–2005 winter is compared to loss inferred during the cold 1999–2000 Arctic winter. These inferred O<sub>3</sub> loss calculations, as well as the observations of O<sub>3</sub> itself, are compared to simulations from the SLIMCAT CTM to deduce how well the dynamics and chemistry were simulated for the 2004–2005 Arctic winter.

## 2. Data Sets

[4] In this section the five satellite data sets that were analyzed for the 2004–2005 Arctic winter are described.

### 2.1. POAM III

[5] POAM III (hereafter referred to as POAM) is a nine-channel solar occultation photometer that was launched in March 1998; the instrument ceased operations in December of 2005 because of an instrument anomaly. POAM has channels ranging from 0.353 to 1.02  $\mu\text{m}$  and measures vertical profiles of O<sub>3</sub>, NO<sub>2</sub>, H<sub>2</sub>O, and aerosol extinction [*Lucke et al.*, 1999]. Because of the sun-synchronous polar orbit, 14–15 POAM observations occur around a circle of latitude in each hemisphere each day, with Northern Hemisphere latitudinal coverage varying slowly between 55°N and 73°N. During the Arctic winter, POAM sampled both inside and outside the polar vortex. For this analysis POAM version 4.0 retrievals, which have a vertical resolution of approximately 1 km in the stratosphere, are used. Version 4.0 O<sub>3</sub> data have changed little from version 3.0, which was validated by *Randall et al.* [2003]; POAM O<sub>3</sub>

measurements agree to within  $\pm 5\%$  with correlative ozone-sonde and satellite data between 13 and 60 km.

### 2.2. SAGE III

[6] SAGE III (hereafter referred to as SAGE) was launched in December 2001, and ceased operations in March of 2006. It utilizes solar occultation to measure vertical profiles of O<sub>3</sub>, NO<sub>2</sub>, H<sub>2</sub>O, temperature, pressure, and aerosol extinction [*Chu et al.*, 2002; *Thomason and Taha*, 2003; *Wang et al.*, 2006]. SAGE uses a grating spectrometer with spectral channels ranging from 280 to 1545 nm. SAGE was launched into a sun-synchronous orbit and its Northern Hemisphere observations range between 50° and 80°N. Atmospheric profiles of O<sub>3</sub> are sampled with  $\sim 0.5$  km vertical resolution in the lower stratosphere. As shown by *Wang et al.* [2006], “the agreement between SAGE and correlative measurements is approximately 5% down to 17 km”. For this work, version 3.0 SAGE data have been used in the comparisons.

### 2.3. EOS MLS

[7] EOS MLS was launched in July 2004. The EOS MLS instrument is composed of heterodyne radiometers operating in 5 spectral regions: 118 GHz, 190 GHz, 240 GHz, 640 GHz, and 2.5 THz [*Waters et al.*, 2006]. EOS MLS measures limb emission at these wavelengths to obtain vertical profiles of a number of species that are relevant to polar studies including temperature, H<sub>2</sub>O, HNO<sub>3</sub>, O<sub>3</sub>, HCl, ClO, and N<sub>2</sub>O. The NASA Aura satellite that hosts the EOS MLS instrument is in a near-polar, sun-synchronous orbit. On each orbit, EOS MLS observations span from 82°S to 82°N [*Waters et al.*, 2006]. The vertical resolution varies for each species and is approximately 2.7 km for O<sub>3</sub> in the lower stratosphere [*Froidevaux et al.*, 2006].

### 2.4. ACE-FTS and MAESTRO

[8] The Atmospheric Chemistry Experiment (ACE) satellite was launched in August 2003. Two solar occultation instruments are included on ACE, the ACE-FTS and MAESTRO instruments. For this work ACE-FTS version 2.2 O<sub>3</sub> update (which compared to versions 1.0 and 2.2 has improved agreement with SAGE, POAM, and ozonesondes near the profile peak) and MAESTRO version 1.1 data are used. ACE-FTS is a high-resolution, Fourier transform infrared spectrometer [*Walker et al.*, 2005] that operates in the 2 to 13 micron spectral region. It measures the vertical distribution of many constituents relevant to polar studies, including temperature, O<sub>3</sub>, H<sub>2</sub>O, CH<sub>4</sub>, NO, NO<sub>2</sub>, HNO<sub>3</sub>, HCl, N<sub>2</sub>O<sub>5</sub>, and ClONO<sub>2</sub> with a vertical resolution of approximately 4 km in the lower stratosphere [*Bernath et al.*, 2005]. MAESTRO is an optical spectrometer covering the 400 to 1030 nm spectral region with a vertical resolution of approximately 1 km; it measures vertical profiles of O<sub>3</sub>, NO<sub>2</sub>, and aerosol extinction.

[9] As indicated above each instrument has a different vertical resolution for the O<sub>3</sub> observations. For this study, all observations and the CTM have been interpolated to a standard potential temperature grid corresponding to a vertical resolution of about 1 km. Before conducting the analysis, the original profiles were compared to the interpolated profiles to ensure that the vertical structure of the profile was not compromised by the interpolation. Implica-

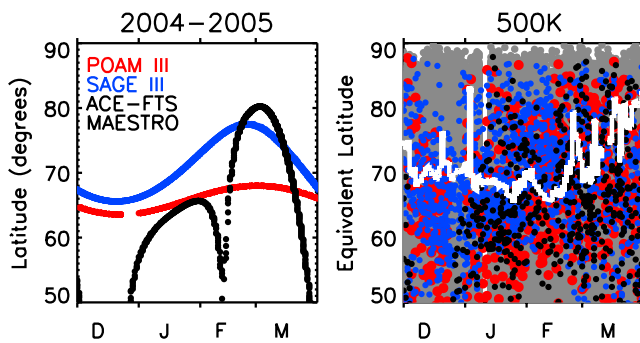


**Figure 1.** Latitudinal coverage for POAM III (red), SAGE III (blue), MAESTRO (black), and ACE-FTS during the 2004–2005 Arctic winter (left). (right) Equivalent latitudes of observations on the 500 K potential temperature surface, applying the same color arrangement used in Figure 1, left, with EOS MLS (gray). White line indicates the innermost edge of the polar vortex.

tions of the different vertical resolutions for the conclusions drawn here are discussed below.

### 2.5. Satellite Comparisons During the 2004–2005 Winter

[10] Figure 1, left, shows the latitude sampling for POAM, SAGE, MAESTRO, and ACE-FTS between 50° and 90°N during the 2004–2005 winter. EOS MLS has been omitted here because of the large number of observations made by the instrument. In the Northern Hemisphere, EOS MLS (not shown), SAGE, and POAM made observations poleward of 60°N from December through mid-April, while MAESTRO and ACE-FTS only sampled air poleward of 60°N from January through early February and from late February through early April. Figure 1, right, shows the equivalent latitudes of all the observations made between 50° and 90°N on the 500 K potential temperature surface during the same period. Equivalent latitude, originally defined by *Butchart and Remsberg* [1986], is a vortex-centered coordinate system where 90° is always in the center of the vortex. The Arctic vortex is often displaced from the pole; therefore conventional zonal means obscure dynamical features by averaging air that is inside and outside the vortex; thus equivalent latitude is used here. The equivalent latitude was calculated from potential vorticity (PV), which was computed from the European Centre for Medium-Range Weather Forecasts (ECMWF) operational analyses. The equivalent latitude was then interpolated from the ECMWF model grid to the observation locations. The vortex algorithm of *Harvey et al.* [2002] was applied to calculate the edge of the Arctic vortex. This algorithm integrates  $Q$ , a strain/rotation parameter around stream function isopleths in each hemisphere.  $Q$  is negative (positive) in flows dominated by rotation (shear).  $Q$  is negative inside the center of the vortex and becomes positive toward the edge with large gradients near the polar night jet. Neighboring stream function contours where  $Q$  changes sign are vortex edge candidates. Of these candidates, the stream function contour with the largest integrated wind speed is defined as the vortex edge (see *Harvey et al.* [2002] for further details). This vortex edge definition agrees well

with algorithms by *Waugh and Randel* [1999] and *Nash et al.* [1996]. The white line in Figure 1, right, denotes the vortex edge as determined using this criterion. Figure 1, right, shows that SAGE, EOS MLS, and POAM sampled air within the vortex throughout most of the Arctic winter. SAGE and POAM observations inside the vortex were located mostly near the edge in middle to late December, and SAGE measurements inside the vortex in February and March were more sporadic than in January. ACE-FTS and MAESTRO only sampled vortex air (i.e., air inside the vortex) from early January through late March, with fewer measurements inside the vortex in early February.

### 3. Methods

[11] To quantify  $O_3$  loss from satellite observations, the “passive subtraction” technique has been used. In this technique, a passive  $O_3$  tracer field, which represents the change in  $O_3$  due to dynamics (horizontal mixing and descent), is subtracted from the observations to quantify the change in  $O_3$  due to chemistry [*Manney et al.*, 1995a, 1995b, 2003; *Goutail et al.*, 2005; *Deniel et al.*, 1998; *Hoppel et al.*, 2002; *Singleton et al.*, 2005]. This technique, which has been widely used and compared favorably with other  $O_3$  loss methods [e.g., *Harris et al.*, 2002; *WMO*, 2003], was applied to the five data sets discussed above. Here we used the University of Leeds SLIMCAT CTM [*Feng et al.*, 2005] (see *W. Feng et al.*, Large chemical ozone loss in 2004/05 Arctic winter/spring, submitted to *Geophysical Research Letters*, 2006, hereinafter referred to as *FE*, submitted paper, 2006) to simulate a global, passive  $O_3$  tracer. The passive  $O_3$  tracer field was then linearly interpolated from the model grid ( $2.8^\circ \times 2.8^\circ$ ) to each satellite measurement location. The inferred  $O_3$  loss (IL) at each measurement location is calculated as the difference between the satellite observation and the modeled passive  $O_3$ ; hereafter this technique is referred to as “CTM passive subtraction” (CTM-PS) [*Singleton et al.*, 2005]. Unlike the study of *Singleton et al.* [2005], which utilized two different methods to quantify the chemical  $O_3$  loss, only one method is used here. The full chemical model was also sampled at each observation location and the difference between the full model and the passive tracer is referred to as the modeled or simulated chemical  $O_3$  loss (ML). The IL and ML were calculated at the satellite observation locations that were inside the vortex, as determined using the vortex criteria of *Harvey et al.* [2002]. Loss calculations were not extended below 400 K because of uncertainties in the identification of the vortex edge due to contamination from the presence of the subtropical jet [*Harvey et al.*, 2002] and the increased influence of mixing [e.g., *McIntyre*, 1995].

[12] The SLIMCAT CTM is a 3-D offline model with detailed stratospheric chemistry, which includes heterogeneous chemistry on solid and liquid aerosols. A full description of the model can be found in *Chipperfield* [1999] and detailed adjustments to the model chemistry and transport are discussed in *Feng et al.* [2005] and *FE*, submitted paper, 2006. The SLIMCAT CTM uses a hybrid sigma-theta grid, with isentropic coordinates in the stratosphere [see *Chipperfield*, 2006]. The run used here extends from the Earth’s surface to approximately 55 km and has a vertical resolution of approximately 2 km in the lower

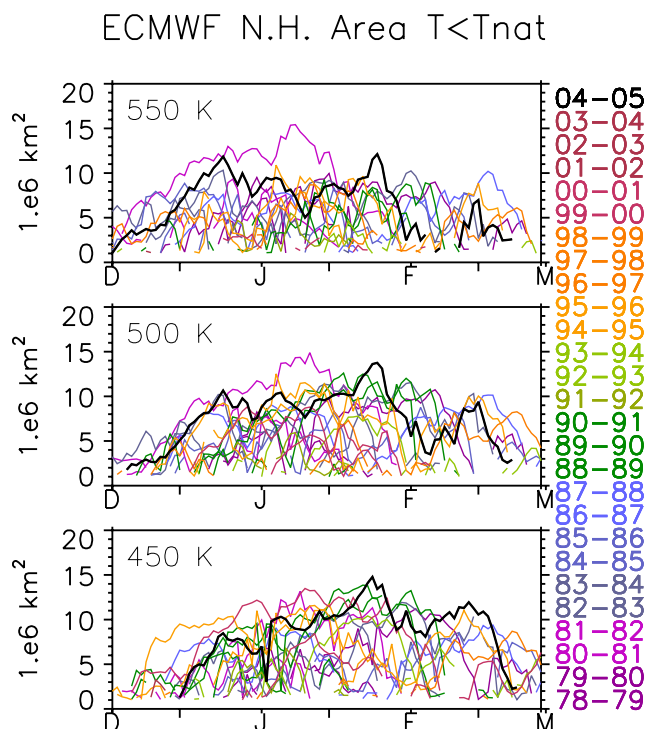


**Figure 2.** Area ( $10^6$  km<sup>2</sup>) where Northern Hemisphere temperatures fell below  $T_{\text{NAT}}$  during the winters from 1978–1979 to 2003–2004 (colors) and for 2004–2005 (black) for the 550 K, 500 K, and 450 K potential temperature surfaces.

stratosphere. For the 2004–2005 simulation, the model temperatures and horizontal winds were forced by ECMWF operational analyses. The NCAR CCM radiation scheme [Briegleb, 1992] was used to handle vertical transport above 350 K.

[13] For this work, a low-resolution ( $7.5 \times 7.5^\circ$ ) run was started on 1 January 1977 and forced with ECMWF ERA-40 and operational analyses. A high-resolution ( $2.8 \times 2.8^\circ$ ) model run was initialized in November 2004 from the low-resolution run. The same SLIMCAT CTM initialization of FE (submitted paper, 2006) has been applied in this work. Values of tropospheric source gases (e.g., CH<sub>4</sub>, N<sub>2</sub>O, and halocarbons) have been set on the basis of WMO [2003] (see also FE, submitted paper, 2006). The model was then integrated through the 2004–2005 Arctic winter with daily meteorological input files from the ECMWF operational analyses.

#### 4. Meteorology

[14] The 2004–2005 Arctic winter was one of the coldest winters recorded in the Arctic [e.g., Manney *et al.*, 2006]. Figure 2 shows the area in the Northern Hemisphere from 1978 through 2005 during the months from December through February where temperatures fell below the nitric acid trihydrate ( $T_{\text{NAT}}$ ) formation temperatures. Temperatures prior to 2000 were taken from ECWFW ERA-40 reanalysis, while temperatures after this year were taken from ECMWF operational analyses. Although ERA-40 has a bias in temperature with respect to other analyses, it

correctly handles interannual variability [e.g., Manney *et al.*, 2005; Tilmes *et al.*, 2006]. A daily averaged  $T_{\text{NAT}}$  value was computed using the Hanson and Mauersberger [1988] expression, where average vortex HNO<sub>3</sub> and H<sub>2</sub>O values were taken from the 2004–2005 SLIMCAT CTM run. These calculations were conducted for the 550 K, 500 K, and the 450 K potential temperature surfaces. Throughout most of the winter, the 2004–2005  $T_{\text{NAT}}$  areas are at the high end of the range shown here. At all three potential temperature levels 2004–2005 had the largest area with temperatures below  $T_{\text{NAT}}$  in late January. There was also another period at 450 K in mid-February where the 2004–2005 winter had the largest possible PSC formation area since 1978. The 2004–2005 Arctic winter vortex enclosed a volume of air where temperatures fell below  $T_{\text{NAT}}$  that was larger than previously observed (e.g., Tilmes *et al.* [2006] and Rex *et al.* [2006]). This diagnostic is a measure of the probability of PSC formation, which is positively correlated with column O<sub>3</sub> loss.

[15] To examine the 2004–2005 meteorology more closely, Figure 3 shows the difference between the minimum ECMWF operational temperatures found inside the vortex at the satellite measurement locations and the daily average  $T_{\text{NAT}}$  (calculated same as above) for the 600 K, 500 K, 450 K, and 425 K potential temperature surfaces. Of all of the instruments, EOS MLS sampled air that experienced the lowest temperatures. Because of the large sampling of the instrument, the EOS MLS temperatures are most representative of the overall minimum temperatures found inside the vortex. Since the other instruments sampled air masses with higher temperatures, this suggests that the other instruments did not sample air in the center of the vortex cold pool. From December through the end of February temperatures

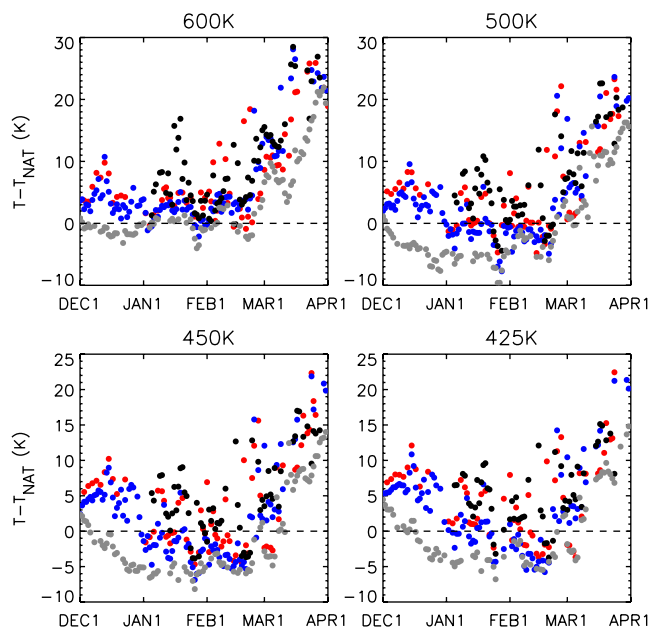


**Figure 3.** Minimum ECMWF operational temperatures minus daily average  $T_{\text{NAT}}$  (see text) inside the vortex at the EOS MLS (gray), ACE-FTS (black), MAESTRO (black), POAM III (red), and SAGE III (blue) measurement locations on the 600 K, 500 K, 475 K, and 425 K potential temperature surfaces during the 2004–2005 Arctic winter.

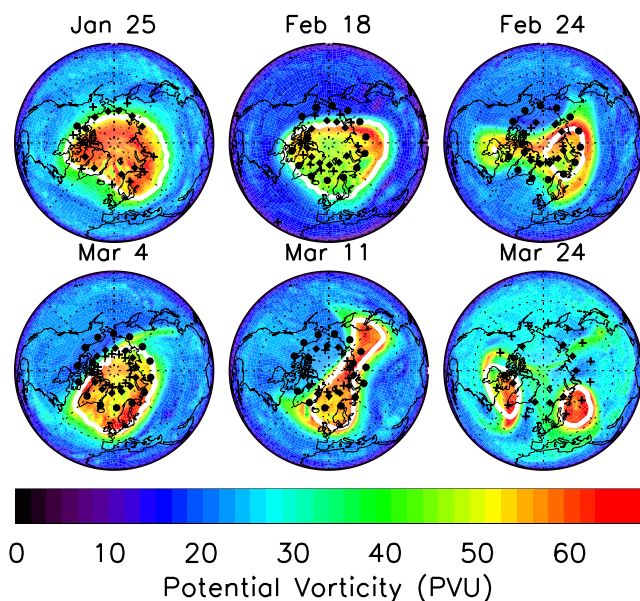


**Figure 4.** ECMWF operational PV ( $10^{-6} \text{ K m}^2 \text{ kg}^{-1} \text{ s}^{-1}$ ) on the 500 K surface for representative days during the 2004–2005 Arctic winter. Inner vortex edge is denoted by the white contour. The POAM III, SAGE III, ACE-FTS, and MAESTRO measurement locations are indicated with circles, diamonds, and crosses, respectively. Latitudes range from the equator to the pole, with latitude circles drawn in 45 degree increments.

at the instrument locations often fell below  $T_{\text{NAT}}$ , with the exception of the ACE instruments, which either did not sample inside the vortex or were at lower geographic latitudes (in early January). Temperatures dramatically increased by March at all of the measurement locations and never returned to the  $T_{\text{NAT}}$  levels due to the onset of a “major final warming” [Manney *et al.*, 2006].

[16] Even though the Arctic region was unusually cold in 2004–2005, the polar vortex was dynamically active [Manney *et al.*, 2006; Schoeberl *et al.*, 2006]. Figure 4 shows ECMWF PV and the vortex edge computed by the

vortex determination criteria of Harvey *et al.* [2002] on the 500 K potential temperature surface for selected representative days. SAGE, POAM, ACE-FTS, and MAESTRO measurement locations are superimposed. From December through mid-February the vortex remained intact. On 24 February, a warming occurred in the lower stratosphere (see Figure 2) that caused a localized split in the vortex; by 1 March the vortex had reformed. However, by mid-March the major final warming caused the vortex to split throughout the depth of the stratosphere and it remained split throughout March. Between January and March the vortex often traversed to lower latitudes, which allowed for more sunlight exposure and thus greater potential for  $\text{O}_3$  loss.

## 5. Results

### 5.1. Inferred $\text{O}_3$ Loss

[17] In order to quantify the IL, the passive model field was interpolated to the satellite measurement locations inside the polar vortex. Daily average profiles of IL for each of the satellite instruments are shown in Figure 5. For qualitative purposes, days when the instrument did not sample inside the vortex and days with missing data (see Figure 1) were filled in by a time interpolation. Data in all contour plots presented in this paper have been smoothed using a 7-day running average.

[18] When applying the CTM-PS technique, it is important to analyze the agreement between the model and the observations on the first day of the analysis, 1 December 2004. Any differences at this time will descend in the model during the run in accordance with the model vertical transport. A positive offset (an indication of  $\text{O}_3$  production) or a negative offset (an indication of  $\text{O}_3$  loss) on 1 December would falsely mask or enhance IL calculations on lower potential temperature surfaces at a later date [Singleton *et al.*, 2005]. On 1 December only POAM, SAGE, and EOS MLS were taking observations inside the polar vortex. The IL from these instruments falsely indicates a small loss of approximately 0.2 ppmv on 1 December above 450 K because of an initial mismatch between the model and observations. Below 450 K there was a more significant (false) loss of 0.5 ppmv at the start of the analysis. Typically, air starting below 450 K on 1 December would

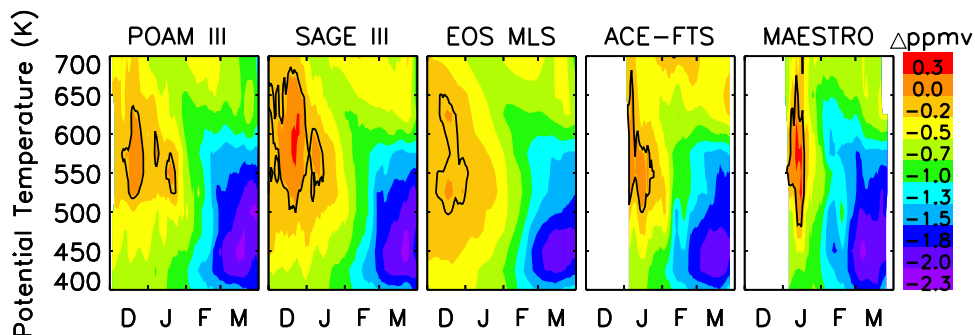


**Figure 5.** Differences (ppmv) between passive  $\text{O}_3$  calculated by the SLIMCAT CTM and  $\text{O}_3$  measured by the POAM III, SAGE III, EOS MLS, ACE-FTS, and MAESTRO instruments. Results correspond to daily averages over the measurement locations inside the vortex during the 2004–2005 Arctic winter and are indicative of inferred photochemical loss throughout the winter. Days with missing data and days where an instrument did not sample the vortex have been filled in with a time interpolation. Solid black line denotes the zero contour. Data have been smoothed with a 7-day running average.

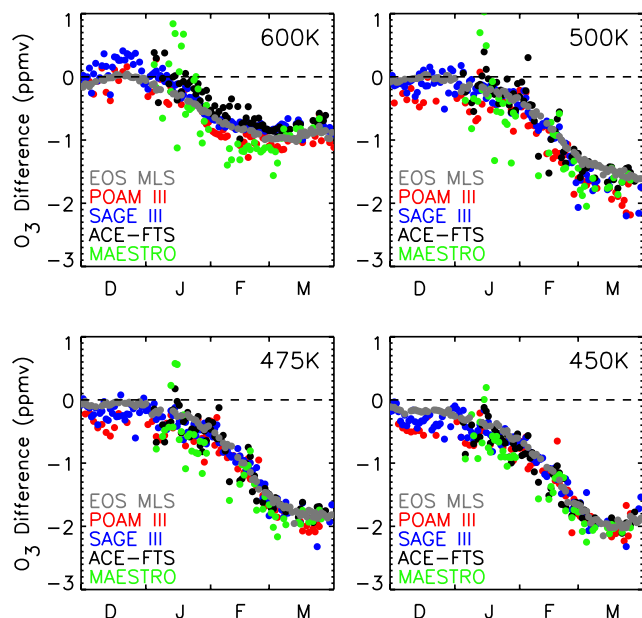


**Figure 6.** Time series of the inferred daily average  $O_3$  loss (ppmv) inside the vortex from EOS MLS (gray), POAM III (red), SAGE III (blue), ACE-FTS (black), and MAESTRO (green) for the 600 K, 500 K, 475 K, and 450 K surfaces during the 2004–2005 Arctic winter.

descend too far (below 400 K, the lower limit of this analysis) during the winter to affect air near levels of peak  $O_3$  loss in March; however, air above 450 K would likely have an impact on  $O_3$  loss calculations inferred at the end of the winter. In this case the offset could lead to an overestimate of loss by up to 0.2 ppmv.

[19] Similar morphology is observed in all of the panels in Figure 5. In particular, loss (relative to the initial offset) begins in early January at the highest potential temperature levels depicted here. In order to determine if this loss is truly chemical or a problem with the modeled dynamics, SLIMCAT and ACE-FTS vortex  $CH_4$  fields were compared (not shown). The  $CH_4$  fields overall show good agreement. During late December through mid-January, the rate of descent in SLIMCAT is somewhat faster than the observations above 550 K. At the same altitudes, signatures consistent with mixing are apparent in both the model and the observations in middle to late January; e.g.,  $CH_4$  increases in time, whereas descent alone would lead to monotonic decreases. Manney *et al.* [2006] also point out that vortex intrusions had occurred during this time as indicated by EOS MLS  $N_2O$  observations. SLIMCAT shows a slightly sharper rise in  $CH_4$  than ACE-FTS, which may indicate the model slightly overestimates mixing compared to the observations. Both of these effects could increase the SLIMCAT passive  $O_3$ , resulting in too much loss at these altitudes. However, Manney *et al.* [2006] show that chlorine activation was observed by MLS above 600 K. Our understanding of this high-altitude loss is thus not complete, and will be a subject for further study. Loss gradually increases at lower potential temperature levels, as depleted air descends in time and additional local

chemical depletion occurs. By late February, loss greater than 1.0 ppmv is inferred throughout the altitude range below 575 K, persisting throughout the month of March. Maximum losses occur near 450 K in mid-March, at values near 2 ppmv. Note that other studies have shown that significant loss occurred during the 2004–2005 Arctic winter below 400 K [von Hobe *et al.*, 2006] [see also Rex *et al.*, 2006], a region not investigated in this study.

[20] A more quantitative diagnosis can be conducted by examining time series of daily averaged IL, which are shown in Figure 6 for the 600 K, 500 K, 475 K, and 450 K surfaces. Unlike Figure 5, days where the instrument did not sample inside the vortex and days with missing data have not been filled in with a time interpolation. Neither ACE-FTS nor MAESTRO sampled vortex air until January. At all levels shown here, IL calculations for the different instruments agree very well, although the solar occultation results are noisier because not as many data points are averaged together compared to EOS MLS (see Figure 1, right, for instrument sampling). Over the range of potential temperature levels considered here, the maximum amount of IL during the 2004–2005 winter occurred between 475 K and 450 K at approximately 2–2.3 ppmv. The IL calculations presented here are comparable to those computed from other techniques. Manney *et al.* [2006] computed EOS MLS IL by analyzing EOS MLS  $N_2O$  observations and vortex-averaged descent rates and found a maximum vortex averaged loss of 1.2–1.5 ppmv between 450 K and 500 K. The same analysis applied to the outer edge of the vortex indicated a maximum loss of  $\sim 2$  ppmv in the same potential temperature region [Manney *et al.*, 2006]. Jin *et al.* [2006] inferred loss from ACE-FTS observations from correlations of  $O_3$  and  $CH_4$ , correlations between  $O_3$  and an artificial tracer, and the profile descent technique. The profile descent technique has also been applied in previous  $O_3$  loss studies, but has been described with different nomenclature [e.g., Larsen *et al.*, 1994; Urban *et al.*, 2004; Raffalski *et al.*, 2005; Manney *et al.*, 2006]. Jin *et al.* [2006] found that the maximum IL occurred between 475 and 500 K and ranged from 1.6–2.3 ppmv. Rex *et al.* [2006] applied the vortex average descent approach to SAGE and POAM data to calculate the accumulated loss between 5 January and 25 March. Compared to the CTM-PS IL results, Rex *et al.* [2006] indicate that the maximum loss occurred at a lower altitude (between 400 and 450 K) and was much less than the CTM-PS. In particular, the vortex average descent approach shows a loss of 1–1.2 ppmv at 500 K for SAGE and POAM, whereas the CTM-PS approach indicates a larger loss of 1.7–2.0 ppmv at this altitude. The vortex average descent approach also shows a larger amount of loss at 450 K compared to 500 K, which is not as pronounced in the CTM-PS IL calculations. However, it is important to point out that accumulated loss calculated by Rex *et al.* [2006] started on a later date than the CTM-PS IL calculations (5 January compared to 1 December). In Figure 6, there is a positive slope in the differences at 600 K between the observations and modeled passive  $O_3$  during December, most evident in the SAGE data. Since  $O_3$  production at 600 K in December is not expected, this suggests a slight error in the passive model calculations. At this level  $O_3$  mixing ratios are generally greater outside the vortex than inside because of poleward transport of  $O_3$  rich

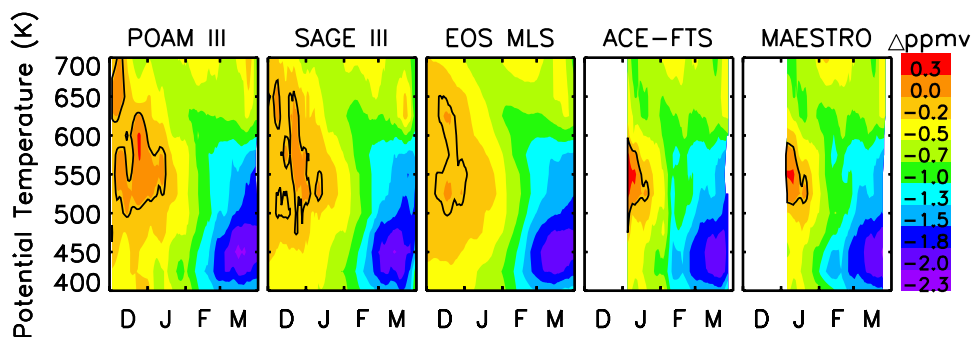


**Figure 7.** As in Figure 5, but using EOS MLS  $O_3$  sampled at the POAM III, SAGE III, ACE-FTS, and MAESTRO instrument locations during the 2004–2005 Arctic winter. The central panel is the same as in Figure 5.

subtropical air [Manney *et al.*, 1995b; Randall *et al.*, 1995; Singleton *et al.*, 2005]. Thus the slope could result from horizontal transport of air from outside the vortex that is not captured by the model. SAGE measurement locations moved equatorward during December, closer to the vortex edge than the other instruments, possibly magnifying any error in the model transport near the vortex edge.

## 5.2. Inferred $O_3$ Loss and Instrument Sampling

[21] As previously mentioned the EOS MLS instrument makes near-global observations on a daily basis, whereas the geographic sampling of the solar occultation instruments is limited to a single latitude circle on any given day. Therefore the EOS MLS IL should more adequately represent true vortex average conditions. However, Figure 1, right, indicates that although the solar occultation instruments have limited geographic sampling, they observed a wide range of equivalent latitudes during the winter; thus in terms of vortex space the solar occultation instruments were not very limited. To examine the sensitivity of the solar occultation IL calculations to limited geographic coverage, we sampled the EOS MLS instrument at the other instrument locations and then calculated the IL. The results of this test are shown in Figure 7. Qualitatively, the IL morphology derived from EOS MLS sampled at the solar occultation locations is the same as derived from the solar occultation instruments themselves. Inferred  $O_3$  loss begins earliest at the highest potential temperature levels, followed by increasing loss at lower levels, with peak loss occurring near 450 K in March. The peak magnitude of the loss inferred from EOS MLS data sampled at the solar occultation locations is only slightly less than that inferred from the solar occultation data themselves.

[22] The similarity between Figures 7 and 5 confirms that the individual differences between each of the panels in Figure 5 are due primarily to differences in geographic sampling. This is expected since  $O_3$  data from most of the instruments have been well validated [e.g., Randall *et al.*, 2003; Wang *et al.*, 2006; Froidevaux *et al.*, 2006] (although see discussion below regarding ACE-FTS versus MAESTRO). EOS MLS has the lowest vertical resolution of all of the instruments tested. Therefore if the vertical resolution had been significant there would have been large discrepancies between Figures 7 and 5. That IL variations from instrument to instrument are generally quite minor (e.g., see Figure 6) leads to the conclusion that even though solar

occultation geographic coverage is limited, the sampling of equivalent latitude can be broad enough to adequately define  $O_3$  loss inside the vortex. Rex *et al.* [2006] also showed little difference in the  $O_3$  loss estimates from sondes, POAM, and SAGE, although the sampling of the instruments in latitude space was quite different. Rex *et al.* [2006] concluded that the similarities in the results increase the confidence that sampling issues do not have a significant impact on the IL calculations.

[23] The ACE-FTS versus MAESTRO comparisons require further explanation. Only preliminary validation has been completed for ACE-FTS version 1.0 data [Walker *et al.*, 2005]; however, detailed studies are in progress for the current versions of both ACE-FTS and MAESTRO data that we use here. Because these instruments are on the same satellite, their geographic sampling is identical. Therefore differences between IL results from these instruments can be attributed to differences in the solar occultation measurements themselves. Indeed, the only reason the Figure 7 EOS MLS plots for the ACE-FTS and MAESTRO sampling are not identical is that days where there is missing ACE-FTS or MAESTRO data (as with all the other instruments) have been filled in with a time interpolation. That the MAESTRO data show more apparent IL in Figure 5 is attributed to the fact that  $O_3$  mixing ratios retrieved from MAESTRO are on average  $\sim 5$ – $10\%$  lower than those retrieved from ACE-FTS, even for coincident data (not shown). However, because of the higher variability in the MAESTRO data, few  $O_3$  measurements near 600 K caused the average vortex MAESTRO  $O_3$  to be slightly higher than the ACE-FTS data in January.

## 5.3. Column $O_3$ Loss

[24] The partial column is the vertical integral of the difference between the observed  $O_3$  and the modeled passive  $O_3$  field [Rex *et al.*, 2002]. The partial column  $O_3$  loss for 2004–2005 is shown in Figure 8. Here the partial column was computed between the potential temperature surfaces of 400 K and 575 K, and only observations where the instruments were sampling within the vortex at all potential temperature levels were used in the calculation. Figure 8 shows that, overall, the partial column  $O_3$  loss is in strong agreement for the five instruments, with maximum loss at the end of March near 100–120 Dobson Units (DU), with an uncertainty of  $\sim 15$  DU. There is an initialization offset between the model and the observations on the first

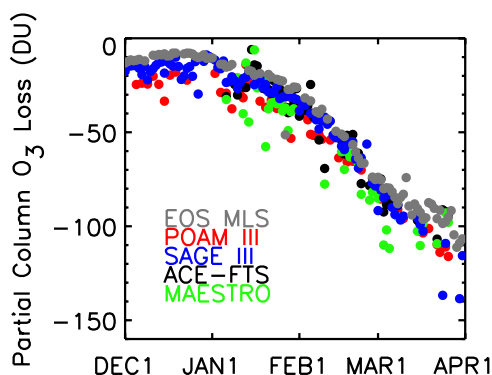


**Figure 8.** Partial column loss for the EOS MLS (gray), POAM III (red), SAGE III (blue), ACE-FTS (black), and MAESTRO (green) instruments between the 575 K and 400 K potential temperature surfaces during the 2004–2005 Arctic winter. Only profiles inside the vortex were included in the calculation.

day of the analysis, representing about 15% of the maximum loss observed. The partial column loss results, once corrected for the initialization offset, agree well with the 90 DU loss calculated by *Rex et al.* [2006] between 400 K and 550 K from ozonesondes (M. Rex, private communication, 2006).

#### 5.4. Comparisons with 1999–2000 IL Calculations

[25] The Arctic  $O_3$  loss which occurred during 2004–2005 was large compared to most previous Arctic winters. One of the coldest observed Arctic winters took place during 1999–2000 [e.g., *WMO*, 2003]. In order to compare the two Arctic winters directly, the CTM-PS technique was applied using the SLIMCAT CTM for the 1999–2000 winter. The same version of the SLIMCAT CTM was used with the 1999–2000 run. Unlike the 2004–2005 run; however, the SLIMCAT CTM was only forced with ECMWF operational winds from January through the remainder of the winter; during December 1999 the CTM was forced with ECMWF ERA-40 winds. Since POAM was the only instrument taking observations in both 2004–2005 and 1999–2000 and because there are in general very few discrepancies in the IL for the five instruments, we compare the 2 years only using POAM data.

[26] Figure 9 shows the time series of the daily averaged IL inside the vortex for the POAM instrument during both of the cold Arctic winters for the 575 K, 550 K, 500 K, and 475 K potential temperature surfaces from 1 December until 15 March. The analysis was only conducted through mid-March because after this time in 2000 the vortex was too close to the pole for POAM to sample [*Hoppel et al.*, 2002; *Rex et al.*, 2002]. Unfortunately, the analysis was not conducted for levels below 475 K because 100 hPa was the lower limit for the 1999–2000 ECMWF operational wind fields that were used to determine the location of the vortex edge. These comparisons are therefore at potential temperature levels above where the maximum loss (in terms of mixing ratio) occurred in both winters [*Rex et al.*, 2006]. *Rex et al.* [2006] applied the vortex average descent approach between 5 January and 25 March to SAGE, POAM, and ozonesondes in 2006 and to ozonesondes in 2000, and showed that the 2005 loss below 475 K was as large as or larger than the loss

that occurred in 2000. Above 475 K, differences between CTM-PS and *Rex et al.* [2006] are expected because of the differences in the time period over which the loss calculations were made. Figure 9 reveals that on the 575 K and 550 K potential temperature surfaces the 2004–2005 calculations show slightly more loss than the 1999–2000 calculations during March. *Rex et al.* [2006] also show that there was more loss in March during 2005 than in 2000 at 550 K, but indicate up to 1 ppmv less accumulated loss occurred in both years compared to the CTM-PS results. The reverse occurs on the 500 K and 475 K surfaces, as shown in Figure 9, where the 1999–2000 winter shows slightly more loss in March, by approximately 0.2 and 0.5 ppmv, respectively. *Rex et al.* [2006] indicate a larger difference between the years at 475 K, with 0.9 ppmv more loss during 2000 than in 2005. Figure 9 indicates that early in the winter (mid-December through the end of January) more loss occurred during 1999–2000 than in 2004–2005 between 475 K and 575 K (the upper reaches of chemical  $O_3$  loss). We speculate that this is due to the fact that 2004–2005 was more dynamically active than 1999–2000 [*Manney et al.*, 2006; *Salawitch et al.*, 2002]. Our understanding of these differences is not complete, and will be a subject for further study. These results agree with those presented by *Rex et al.* [2006] and *Manney et al.* [2006], which show that more loss occurred during 2000 at 500 K and 475 K than in 2005.

#### 5.5. Modeled $O_3$ Loss

[27] The SLIMCAT CTM ML was analyzed to determine how well the model was able to reproduce the 2004–2005 Arctic  $O_3$  loss inferred from the observations. A contour plot of the daily average ML is shown in Figure 10. In order

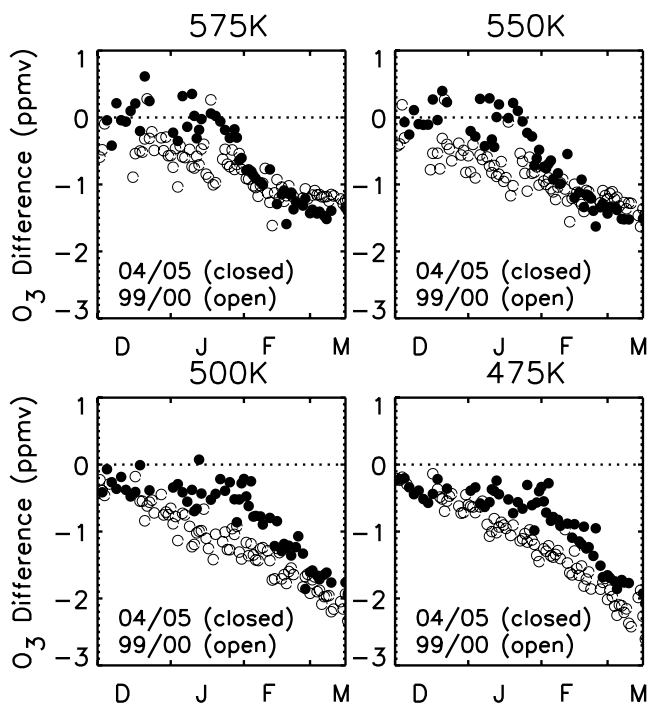


**Figure 9.** Time series of the inferred daily average  $O_3$  loss (ppmv) for POAM III during the 2004–2005 (closed circles) and the 1999–2000 (open circles) Arctic winters. Inferred loss is shown for 1 December through 15 March for the 575 K, 550 K, 500 K, and 475 K surfaces.

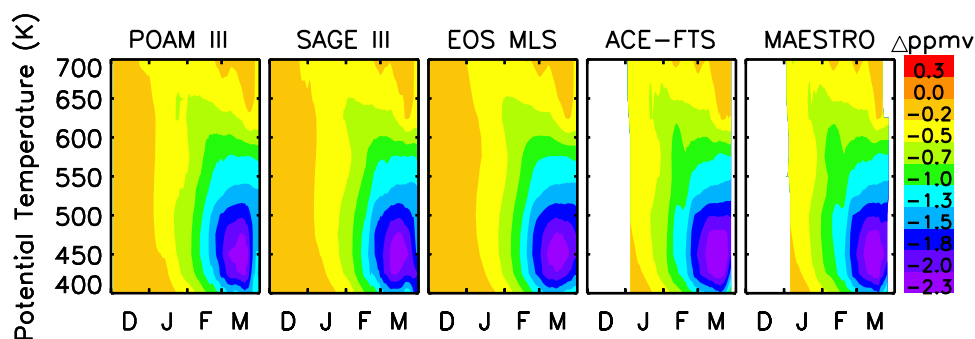


**Figure 10.** As in Figure 5, but for modeled daily average  $O_3$  loss (ppmv) inside the vortex at the POAM III, SAGE III, EOS MLS, ACE-FTS, and MAESTRO locations during the 2004–2005 Arctic winter.

to compute the ML, the SLIMCAT CTM was sampled at each of the satellite measurement locations. As in Figure 5, data on days where there was missing satellite data and on days where the instrument did not sample inside the vortex are filled in by a time interpolation. Both the IL and ML show strong descent of  $O_3$  loss starting near 700 K in December and peaking below 500 K by mid-March. Above 500 K the ML slightly underestimates the magnitude of the IL starting in February. The amount by which the model underestimates the loss varies for each instrument. The opposite is true below 500 K, where the ML calculations show a peak loss that is larger in magnitude by about 0.3 ppmv than the peak IL values at these potential temperature levels. At 450 K the ML diverges from the IL calculations starting in late February, when the major final warming occurred. This suggests the possibility that the model had difficulty simulating the effects of the stratospheric warming event. Despite these differences, qualitatively the ML agrees well with the IL calculations.

### 5.6. Satellite $O_3$ and CTM Active $O_3$

[28] The differences between the ML and the IL calculations are due to differences between the satellite  $O_3$  observations and the active (full chemistry and dynamics) model field. If the chemistry, physics and the meteorology in the SLIMCAT CTM were accurate, the active model  $O_3$  should match the observations, within the uncertainties introduced by initialization errors. Figure 11 shows the evolution of daily average vortex  $O_3$  for the observations, the corresponding active model sampled at the observation locations, and the difference (active model  $O_3$  minus observed  $O_3$ ). Time series of the active model and the observations at 600 K and 450 K are shown in Figure 12. Qualitatively, the model simulates the observed  $O_3$  quite well. At these altitudes,  $O_3$  mixing ratios increase with increasing altitude. Between 550 K and 700 K,  $O_3$  mixing ratios increase in time from December to March because of poleward transport of ozone-rich air into the vortex. From about 450–550 K,  $O_3$  mixing ratios decrease in time, as halogen-activated  $O_3$  destruction becomes prevalent. Below 450 K,  $O_3$  mixing ratios increase in December and early January as  $O_3$ -rich air descends; mixing ratios then decrease as halogen-activated chemistry takes over.

[29] One notable feature in Figure 11 is the small model underestimate of  $O_3$  that descends in time throughout the winter; this is surrounded at lower and higher altitudes by model overestimates of the observed  $O_3$  field. The over-

estimates at the beginning of the winter are correlated with initialization errors, and cannot be interpreted as indicating any errors in the model chemistry or physics. The precise magnitude and altitude of the underestimate (blue region in Figure 11) varies with instrument and time, but in general is on the order of 0.3 ppmv or less, and descends from about 550–600 K in December to about 400–450 K in mid-March. The underestimate is on average smaller when compared to EOS MLS data, which may in part be due to the fact that averaging large numbers of data points masks any initialization errors that might be present at given latitudes. Since the model  $O_3$  underestimates occur near the primary altitudes/times of halogen-activated  $O_3$  loss, they most likely result from small discrepancies between the simulated and observed relative contributions of transport and chemistry to the overall  $O_3$  variations. The results from Figure 12 are particularly interesting at 450 K, where the model overestimates  $O_3$  in December and January, but then underestimates  $O_3$  in March. As noted above, the initial overestimate is clearly related to an initialization error, as it occurs even in early December. The fact that this then transitions to an underestimate explains the larger ML compared to the IL. The differences between the model and observations in March are not well understood. They may be due to the fact that the model did not properly simulate the impact of the final stratospheric warming event. That is, it is possible that the model was too diffusive in the lower stratosphere and allowed low  $O_3$  from outside the vortex to mix into the vortex, resulting in  $O_3$  mixing ratios that were too low. SLIMCAT and ACE-FTS vortex averaged  $CH_4$  mixing ratios (not shown) increase in time during March below 500 K, consistent with increased mixing. EOS MLS  $N_2O$  observations presented in Manney *et al.* [2006] also confirm that mixing was occurring during this time. As with the higher altitudes,  $CH_4$  mixing ratios in SLIMCAT increase more than those in ACE-FTS, which may be a signature of mixing that is not accounted for properly in the model. The differences in March may also be due to the model overestimating the chemical loss because of too strong denitrification, which would allow high  $ClO_x$  to persist longer (M. P. Chipperfield, private communication, 2006).

## 6. Summary and Conclusions

[30] We have presented an overview of the  $O_3$  loss during the 2004–2005 Arctic winter using the CTM-PS technique.

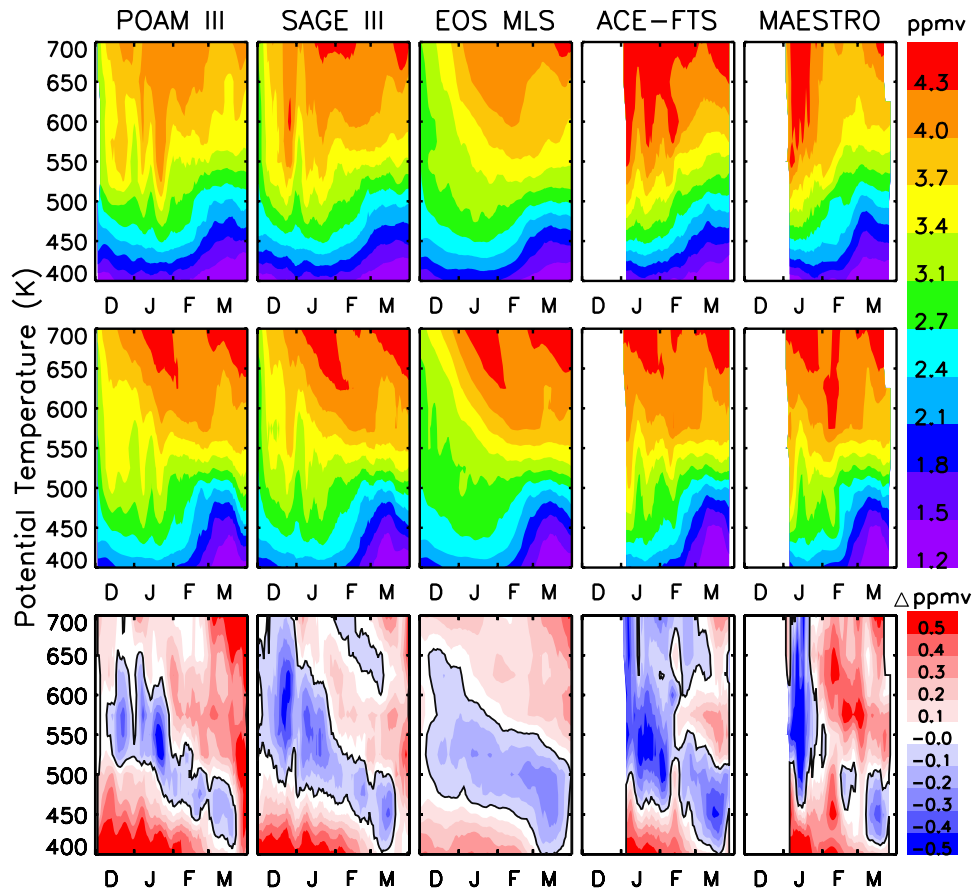


**Figure 11.** Daily average vortex O<sub>3</sub> (ppmv) during the 2004–2005 Arctic winter for (top) POAM III, SAGE III, EOS MLS, ACE-FTS, and MAESTRO, (center) the SLIMCAT active model interpolated to the satellite locations, and (bottom) the SLIMCAT active model minus the observations. Days with missing data and days where an instrument did not sample the vortex have been filled in with a time interpolation. Data have been smoothed with a 7-day running average.

The 2004–2005 winter had lower temperatures than most previously recorded Arctic winters [Manney *et al.*, 2006; Jin *et al.*, 2006; Rex *et al.*, 2006; FE, submitted paper, 2006] and had a dynamically active vortex. During the winter the vortex experienced two warming events. The first event occurred in late February and split the vortex in the lower

stratosphere. In addition to weakening the vortex, the warming event caused the vortex to be stretched and brought down to lower latitudes. The vortex reformed in a couple of days and remained intact until the major final warming event occurred in early to mid-March [Manney *et al.*, 2006] and split the vortex through the depth of the

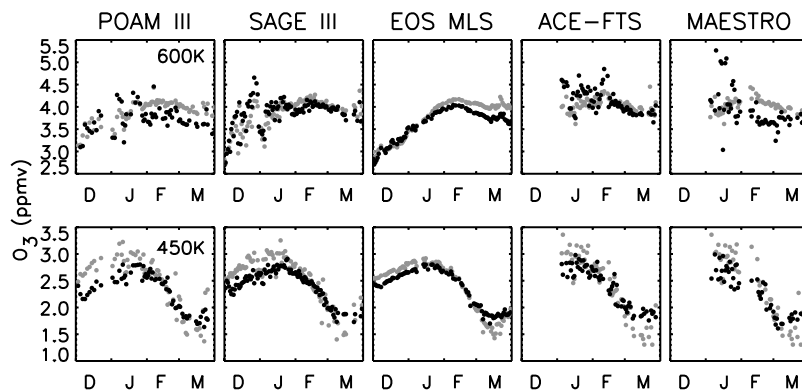


**Figure 12.** Observed (black) and modeled (gray) daily average O<sub>3</sub> (ppmv) inside the vortex for POAM III, SAGE III, EOS MLS, ACE-FTS, and MAESTRO on the 600 K (top) and 450 K (bottom) potential temperature surfaces during the 2004–2005 Arctic winter.

stratosphere. After the first warming event the temperatures warmed and never fell below  $T_{\text{NAT}}$  for the remainder of the winter.

[31] The 2004–2005 Arctic winter was unique because of the large number of satellite observations made. Here we have employed observations from the POAM, SAGE, EOS MLS, ACE-FTS, and MAESTRO satellite instruments. The low temperatures experienced during the winter allowed for prime conditions for chemical  $\text{O}_3$  loss. The inferred loss calculations show similar morphology for all of the instruments. The peak inferred loss occurred for each instrument at approximately 450 K in mid-March at a value of approximately 2–2.3 ppmv. A slight offset between the passive model and SAGE, POAM, and EOS MLS data on 1 December may cause an overestimate of the loss by approximately 0.2 ppmv. Maximum  $\text{O}_3$  loss calculations are comparable to calculations of FE (submitted paper, 2006) and to outer vortex calculations of Manney *et al.* [2006], but are slightly larger than Rex *et al.* [2006]. Partial column loss results agree well with ozonesonde calculations of Rex *et al.* [2006] between 400 K and 550 K (M. Rex, private communication, 2006). Because each instrument had different latitudinal sampling of the vortex, we were able to evaluate the sensitivity of the inferred loss calculation to the geographic sampling of the instrument. The results suggest that although the solar occultation instruments have limited geographic sampling they do observe a wide range of equivalent latitudes during the winter and therefore are able to adequately sample the vortex for  $\text{O}_3$  loss studies.

[32] In this study we calculated the modeled loss from the SLIMCAT CTM and compared the results to IL calculations to determine how well the CTM was able to simulate  $\text{O}_3$  loss during the 2004–2005 Arctic winter. The SLIMCAT CTM modeled loss had a morphology similar to that of the inferred loss calculations. In the past, CTMs have underestimated  $\text{O}_3$  loss compared to loss inferred from observations [Chipperfield *et al.*, 1996; Deniel *et al.*, 1998; Becker *et al.*, 2000; Guirlet *et al.*, 2000]. Unlike earlier versions of the SLIMCAT CTM, this version no longer underestimates the loss. On the contrary, the CTM slightly overestimates the loss by approximately 0.3 ppmv ( $\sim 10$ – $15\%$ ) after 1 March between 450 and 500 K, but overall the modeled loss agrees very well with the inferred loss calculations. Future work will involve comparing other retrieved satellite species to the model in order to fully test the model's ability to simulate the chemistry and dynamics of the 2004–2005 Arctic winter. This study and the study of Singleton *et al.* [2005] have shown that the SLIMCAT CTM was able to reproduce the maximum loss inferred from satellite observations for both the 2002–2003 and 2004–2005 Arctic winters using the CTM passive subtraction technique to within 15%. Although some discrepancies between the observed and modeled  $\text{O}_3$  remain (such as  $\text{O}_3$  loss above 550 K), the level of agreement has improved from previous studies. Thus these results help to increase confidence in our understanding of Arctic  $\text{O}_3$  loss processes.

[33] **Acknowledgments.** This research is supported by the NASA Earth System Science Fellowship Program, the NASA SOSST Program, and the Aura/HIRDLS Program. Work at the Jet Propulsion Laboratory, California Institute of Technology, was done under contract with the National Aeronautics and Space Administration. The ACE mission is

supported by funding from the Canadian Space Agency, the Natural Sciences and Engineering Research Council of Canada, and the Canadian Foundation for Climate and Atmospheric Sciences. The SLIMCAT modeling work was supported by the EU SCOUT-O3 Project. We thank two anonymous reviewers for helpful comments on this manuscript. C.S.S. thanks Patricia Weis-Taylor, Ph.D., for helpful discussions.

## References

- Becker, G., R. Müller, D. S. McKenna, M. Rex, K. Carslaw, and H. Oelhaf (2000), Ozone loss rates in the Arctic stratosphere in the winter 1994–1995: Model simulations underestimate results of the Match analysis, *J. Geophys. Res.*, **105**, 15,175–15,184.
- Bernath, P. F., et al. (2005), Atmospheric Chemistry Experiment (ACE): Mission overview, *Geophys. Res. Lett.*, **32**, L15S01, doi:10.1029/2005GL022386.
- Briegleb, B. P. (1992), Delta-Eddington approximation for solar radiation in the NCAR community climate model, *J. Geophys. Res.*, **97**(D7), 7603–7612.
- Butchart, N., and E. E. Remsburg (1986), The area of the stratospheric polar vortex as a diagnostic for tracer transport on an isentropic surface, *J. Atmos. Sci.*, **43**, 1319–1339.
- Chipperfield, M. P. (1999), Multiannual simulations with a three-dimensional chemical transport model, *J. Geophys. Res.*, **104**(D1), 1781–1806.
- Chipperfield, M. P. (2006), New version of the TOMCAT/SLIMCAT offline chemical transport model: Intercomparison of stratospheric tracer experiments, *Q. J. R. Meteorol. Soc.*, **132**, 1179–1203.
- Chipperfield, M. P., A. M. Lee, and J. A. Pyle (1996), Model calculations of ozone depletion in the Arctic polar vortex for 1991/92 to 1994/95, *Geophys. Res. Lett.*, **23**, 559–562.
- Chu, W. P., C. R. Trepte, R. E. Veiga, M. S. Cisewski, and G. Taha (2002), SAGE III measurements, *Proc. SPIE Int. Soc. Opt. Eng.*, **48**, 457–464.
- Deniel, C., R. M. Bevilaqua, J. P. Pommereau, and F. Lefèvre (1998), Arctic chemical ozone depletion during the 1994–1995 winter deduced from POAM II satellite observations and the REPROBUS three-dimensional model, *J. Geophys. Res.*, **103**, 19,231–19,244.
- Farman, J. C., B. G. Gardiner, and J. D. Shanklin (1985), Large losses of total ozone in Antarctica reveal seasonal  $\text{ClO}_x/\text{NO}_x$  interaction, *Nature*, **315**, 207–210.
- Feng, W., et al. (2005), Three-dimensional model study of the Arctic ozone loss in 2002/03 and comparison with 1999/2000 and 2003/04, *Atmos. Chem. Phys.*, **5**, 139–152, SRef-ID:1680-7374/acp/2005-5-139.
- Froidevaux, L., et al. (2006), Early validation analyses of atmospheric profiles from EOS MLS on the Aura satellite, *IEEE Trans. Geosci. Remote Sens.*, **44**(5), 1106–1121.
- Goutail, F., et al. (2005), Early unusual ozone loss during the Arctic winter 2002/2003 compared to other winters, *Atmos. Chem. Phys.*, **5**, 665–677.
- Guirlet, M., M. P. Chipperfield, J. A. Pyle, F. Goutail, J. P. Pommereau, and E. Kyrö (2000), Modeled Arctic ozone depletion in winter 1997/1998 and comparison with previous winters, *J. Geophys. Res.*, **105**, 22,185–22,200.
- Hanson, D., and K. Mauersberger (1988), Laboratory studies of the nitric acid trihydrate: Implications for the south polar stratosphere, *Geophys. Res. Lett.*, **15**, 855–858.
- Harris, N. R. P., M. Rex, F. Goutail, B. M. Knudsen, G. L. Manney, R. Müller, and P. von der Gathen (2002), Comparison of empirically derived ozone losses in the Arctic vortex, *J. Geophys. Res.*, **107**(D20), 8264, doi:10.1029/2001JD000482.
- Harvey, V. L., R. B. Pierce, T. D. Fairlie, and M. H. Hitchman (2002), A climatology of stratospheric polar vortices and anticyclones, *J. Geophys. Res.*, **107**(D20), 4442, doi:10.1029/2001JD001471.
- Hoppel, K., R. M. Bevilaqua, G. Nedoluha, C. Deniel, F. Lefèvre, J. Lumpe, M. Fromm, C. E. Randall, J. Rosenfield, and M. Rex (2002), POAM III observations of Arctic ozone loss for the 1999/2000 winter, *J. Geophys. Res.*, **107**(D20), 8262, doi:10.1029/2001JD000476.
- Jin, J. J., et al. (2006), Severe Arctic ozone loss in the winter 2004/2005: Observations from ACE-FTS, *Geophys. Res. Lett.*, **33**, L15801, doi:10.1029/2006GL026752.
- Larsen, N., B. Knudsen, I. S. Mikkelsen, T. S. Jørgensen, and P. Eriksen (1994), Ozone depletion in the Arctic stratosphere in early 1993, *Geophys. Res. Lett.*, **21**(15), 1611–1614.
- Lucke, R. L., et al. (1999), The polar ozone and aerosol measurement (POAM) III instrument and early validation results, *J. Geophys. Res.*, **104**, 18,785–18,799.
- Manney, G. L., et al. (1995a), Lagrangian transport calculations using UARS data, part I: Passive tracers, *J. Atmos. Sci.*, **52**, 3049–3068.
- Manney, G. L., R. W. Zurek, W. A. Lahoz, R. S. Harwood, J. B. Kumer, J. Mergenthaler, A. E. Roche, A. O'Neill, R. Swinbank, and J. W. Waters (1995b), Lagrangian transport calculations using UARS data, part II: Ozone, *J. Atmos. Sci.*, **52**, 3069–3081.

- Manney, G. L., L. Froidevaux, M. L. Santee, N. J. Livesey, J. L. Sabutis, and J. W. Waters (2003), Variability of ozone loss during Arctic winter (1991–2000) estimated from UARS Microwave Limb Sounder measurements, *J. Geophys. Res.*, *108*(D4), 4149, doi:10.1029/2002JD002634.
- Manney, G. L., K. Krüger, J. L. Sabutis, S. A. Sena, and S. Pawson (2005), The remarkable 2003–2004 winter and other recent warm winters in the Arctic stratosphere since the late 1990s, *J. Geophys. Res.*, *110*, D04107, doi:10.1029/2004JD005367.
- Manney, G. L., M. L. Santee, L. Froidevaux, K. Hoppel, N. J. Livesey, and J. W. Waters (2006), EOS MLS observations of ozone loss in the 2004–2005 Arctic winter, *Geophys. Res. Lett.*, *33*, L04802, doi:10.1029/2005GL024494.
- McIntyre, M. E. (1995), The stratospheric polar vortex and sub-vortex: Fluid dynamics and midlatitude ozone loss, *Philos. R. Soc. London Ser. A*, *35*, 227–240.
- Nash, E. R., P. A. Newman, J. E. Rosenfield, and M. R. Schoeberl (1996), An objective determination of the polar vortex using Ertel's potential vorticity, *J. Geophys. Res.*, *101*, 9471–9478.
- Raffalski, U., et al. (2005), Evolution of stratospheric ozone during winter 2002/2003 as observed by a ground-based millimetre wave radiometer at Kiruna, Sweden, *Atmos. Chem. Phys.*, *5*, 1399–1407.
- Randall, C. E., et al. (1995), Preliminary results from POAM II: Stratospheric ozone at high northern latitudes, *Geophys. Res. Lett.*, *22*, 2733–2736.
- Randall, C. E., et al. (2003), Validation of POAMIII ozone: Comparisons with ozonesonde and satellite data, *J. Geophys. Res.*, *108*(D12), 4367, doi:10.1029/2002JD002944.
- Rex, M., et al. (2002), Chemical depletion of Arctic ozone in winter 1999/2000, *J. Geophys. Res.*, *107*(D20), 8276, doi:10.1029/2001JD000533.
- Rex, M., et al. (2006), Arctic winter 2005: Implications for stratospheric ozone loss and climate change, *Geophys. Res. Lett.*, *33*, L23808, doi:10.1029/2006GL026731.
- Salawitch, R. J., et al. (2002), Chemical loss of ozone during the Arctic winter of 1999/2000: An analysis based on balloon-borne observations, *J. Geophys. Res.*, *107*(D20), 8269, doi:10.1029/2001JD000620.
- Schoeberl, M. R., et al. (2006), Chemical observations of a polar vortex intrusion, *J. Geophys. Res.*, *111*, D20306, doi:10.1029/2006JD007134.
- Singleton, C. S., C. E. Randall, M. P. Chipperfield, S. Davies, W. Feng, R. M. Bevilacqua, K. W. Hoppel, M. D. Fromm, G. L. Manney, and V. L. Harvey (2005), 2002–2003 Arctic ozone loss deduced from POAM III satellite observations and the SLIMCAT chemical transport model, *Atmos. Chem. Phys.*, *5*, 597–609, SRef-ID:1680-7324/acp/2005-5-597.
- Thomason, L. W., and G. Taha (2003), SAGE III aerosol extinction measurements: Initial results, *Geophys. Res. Lett.*, *30*(12), 1631, doi:10.1029/2003GL017317.
- Tilmes, S., R. Müller, A. Engel, M. Rex, and J. M. Russell III (2006), Chemical ozone in the Arctic and Antarctic stratosphere between 1992 and 2005, *Geophys. Res. Lett.*, *33*, L20812, doi:10.1029/2006GL026925.
- Urban, J., et al. (2004), The Northern Hemisphere stratospheric vortex during the 2002–03 winter: Subsidence, chlorine activation and ozone loss observed by the Odin Sub-Millimetre Radiometer, *Geophys. Res. Lett.*, *31*, L07103, doi:10.1029/2003GL019089.
- von Hobe, M., et al. (2006), Severe ozone depletion in the cold Arctic winter 2004–2005, *Geophys. Res. Lett.*, *33*, L17815, doi:10.1029/2006GL026945.
- Walker, K. A., C. E. Randall, C. R. Trepte, C. D. Boone, and P. F. Bernath (2005), Initial validation comparisons for the Atmospheric Chemistry Experiment (ACE-FTS), *Geophys. Res. Lett.*, *32*, L16S04, doi:10.1029/2005GL022388.
- Wang, H.-J., D. M. Cunnold, C. Trepte, L. W. Thomason, and J. M. Zawodny (2006), SAGE III solar ozone measurements: Initial results, *Geophys. Res. Lett.*, *33*, L03805, doi:10.1029/2005GL025099.
- Waters, J. W., et al. (2006), The Earth Observing System Microwave Limb Sounder (EOS MLS) on the Aura satellite, *IEEE Trans. Geosci. Remote Sens.*, *44*(5), 1075–1092.
- Waugh, D. W., and W. J. Randel (1999), Climatology of Arctic and Antarctic polar vortices using elliptical diagnostics, *J. Atmos. Sci.*, *56*, 1594–1613.
- World Meteorological Organization (WMO) (2003), *Scientific Assessment of Ozone Depletion: 2002, Global Ozone Research and Monitoring Project, Rep. 47*, 498 pp., Geneva.

P. F. Bernath, C. D. Boone, and K. A. Walker, Department of Chemistry, University of Waterloo, Waterloo, Ontario N2L 3G1, Canada.

M. P. Chipperfield and W. Feng, Institute for Atmospheric Science, School of Earth and Environment, University of Leeds, Leeds LS2 9JT, UK.

L. Froidevaux and G. L. Manney, Jet Propulsion Laboratory, California Institute of Technology, Pasadena, CA 91109, USA.

V. L. Harvey, C. E. Randall, and C. S. Singleton, Laboratory for Atmospheric and Space Physics, UCB 392, University of Colorado, Boulder, CO 80309-0392, USA. (cynthia.singleton@lasp.colorado.edu)

K. W. Hoppel, Naval Research Laboratory, Remote Sensing Physics Branch, Code 7220, Building 2, 4555 Overlook Avenue SW, Washington, DC 20375-5351, USA.

C. T. McElroy, Meteorological Service of Canada, Environment Canada, 4905 Dufferin Street, Downsview, ON, Canada, M3H 5T4.